

Excited state preparation on a quantum computer through adiabatic light-matter coupling

Hugh G. A. Burton^{1,*} and Maria-Andreea Filip²

¹*Department of Chemistry, University College London, London, WC1H 0AJ, U.K.*

²*Yusuf Hamied Department of Chemistry, University of Cambridge, Lensfield Road, Cambridge, CB2 1EW, U.K.*

(Dated: December 1, 2025)

Quantum computing has the potential to transform simulations of quantum many-body problems at the heart of electronic structure theory. Efficient quantum algorithms to compute the eigenstates of fermionic Hamiltonians, such as quantum phase estimation, rely critically on high-accuracy initial state preparation. While several state preparation algorithms have been proposed for fermionic ground states, the preparation of excited states remains a major challenge, limiting the applicability of quantum algorithms to photochemistry and photophysics. In this contribution, we describe a physically motivated adiabatic state preparation technique for low-lying excited states using the explicit coupling between electrons and photons. Our approach systematically converges to the first optically accessible excited state and can target different symmetry sectors by changing the photon polarization. We demonstrate the preparation of high-fidelity excited states for the Hubbard model and methylene molecule across a range of correlation regimes, and perform a successful hardware implementation for a model Hamiltonian.

Introduction

Computing excited-state electronic wavefunctions is central to theoretically understanding interactions between light and matter, enabling predictions of optical material properties, absorption and emission spectra, and photochemical reaction pathways. However, excited states are more challenging to solve than ground states because the variational principle generally cannot be used to find the best wavefunction approximation. We currently rely on multiconfigurational theory, which scales exponentially with system size, or linear response methods that can only describe single-electron excitations and are only accurate if a good ground-state approximation can be found.^(1, 2) Accurate excited-state predictions for molecules and materials with strong electron correlation or multi-electron excitations remain a major theoretical challenge.

Electronic structure theory is poised to be one of the first applications of quantum computers, benefiting from the fact that a linear number of qubits can encode the exponentially scaling electronic Hilbert space.^(3–5) The success of both near-term and fault-tolerant quantum algorithms depends on the overlap between an initial trial state $|\Psi_T\rangle$, prepared on the quantum device, and the true eigenstate $|\Psi_I\rangle$ of interest.⁽⁶⁾ For example, the probability of measuring the ground-state energy E_0 using quantum phase estimation scales as $p(E_0) \propto |\langle\Psi_T|\Psi_0\rangle|^2$.⁽⁷⁾ To address this challenge, several high-accuracy state-preparation methods have been established for ground states, including adiabatic state preparation (ASP),^(7, 8) the variational quantum eigensolver (VQE),^(9, 10) and circuits to encode high-accuracy wavefunctions that have been precomputed on a conventional computer.⁽¹¹⁾ In contrast, algorithms to prepare excited states are much less explored and have focused almost exclusively on hybrid VQE methods.^(12–23)

In this work, we introduce an excited state preparation technique that uses quantum adiabatic state preparation to directly convert between ground and excited states by leveraging the physical coupling between photons and electrons. Our approach starts with the electronic ground state $|\Psi_0\rangle$ and a singly-occupied photon state $|1\rangle$ encoded on a quantum register as the multicomponent product state $|\Psi_0\rangle \otimes |1\rangle$. Starting with the initial photon frequency $\omega = 0$, the state is adiabatically evolved while increasing ω and explicitly coupling the electronic and photonic modes through the dipole operator. By following a suitable pathway, the combined state can be continuously evolved into an excited electronic state $|\Psi_{es}\rangle$ coupled to the photon vacuum state, i.e. $|\Psi_{es}\rangle \otimes |0\rangle$. This approach artificially controls the physical coupling between electrons and photons in a photoexcitation, allowing the ground state to be adiabatically evolved into the lowest optically accessible excited state without any prior knowledge of the excited-state wavefunction.

Current excited-state quantum algorithms are primarily based on VQE or quantum subspace diagonalization (QSD) methods. Excited-state VQE algorithms employ modified objective functions, such as the ensemble energy of multiple low-lying states^(12–15) and the folded-spectrum approach,^(16–18) or enforce orthogonality to the ground state and lower-lying excited states.^(19–23) These methods all require a suitable variational *ansatz* and face practical challenges such as difficult convergence, high measurement costs, and deep quantum circuits. Furthermore, the multitude of stationary points in variational algorithms⁽²⁴⁾ may hinder excited-state assignment as the variational principle no longer indicates the most physical approximation. Alternatively, QSD uses the quantum device to compute Hamiltonian and overlap matrix elements for a set of basis states.⁽²⁵⁾ The basis may be constructed using real or imaginary time evolution,^(26, 27) as a Krylov expansion,^(28, 29) or from equation of motion and

* h.burton@ucl.ac.uk

linear response theory.(30–37) This approach has seen significant recent interest in the context of quantum selected configuration interaction and sample-based quantum diagonalization, where the most important electron configurations are sampled from a trial state prepared on the quantum device.(38–42) While solving the subsequent generalized eigenvalue problem provides ground- and excited-state energies, QSD is less suited to excited state preparation because encoding the linear combination of basis states on the quantum device requires many ancilla qubits and controlled operations.(11)

Alternatively, adiabatic state preparation (ASP) is a well-established method for preparing fermionic ground states,(7, 8, 11, 43–46) although it is much less explored than methods based on VQE and QSD. After initialising the quantum state as an eigenstate of a reference Hamiltonian \hat{H}_{init} , for which the ground state can be easily prepared, the system undergoes time evolution as the Hamiltonian is slowly changed to match the target system \hat{H}_{final} . If the time evolution is sufficiently slow, then the adiabatic theorem ensures that the system remains in an eigenstate at all times, becoming the target eigenstate at the end of the evolution.(47) The success of adiabatic time evolution is controlled by the minimum energy gap along the pathway, with a smaller gap requiring longer time evolution.(8) Compared to VQE, adiabatic methods have more robust theoretical guarantees of success and rely on fewer heuristics, such as the definition of a variational ansatz. Previous investigations for quantum chemistry have focussed on ground state preparation, with \hat{H}_{init} defined using a one-body Fock operator(43) or from the diagonal of the many-body Hamiltonian.(7, 44) However, to the best of our knowledge, no ASP algorithms have yet been proposed for excited state preparation.

Here, we describe the Excited Adiabatic State Preparation (EXASP) algorithm to prepare the lowest optically accessible excited state on a quantum computer. We define an adiabatic evolution pathway to construct high-fidelity excited-state wavefunctions on a quantum register and show how the fidelity can be further enhanced using post-measurement selection. Our approach requires minimal prior information about the target excited-state wavefunction and is free from any variational ansatz or diagonalization. Furthermore, we show how specific molecular excited states can be targeted using symmetry selection rules. Our approach can prepare high-accuracy excited states for both weakly and strongly correlated Hamiltonians, and provides a fault-tolerant route towards quantum initial state preparation for theoretical photochemistry.

Results

Excited adiabatic state preparation

The adiabatic theorem states that a system will remain in an instantaneous eigenstate if changes to the Hamiltonian occur sufficiently slowly and there is a non-zero gap between the corresponding eigenvalue and the rest of the spectrum.(47) Quantum adiabatic state preparation exploits this theorem by defining an initial Hamiltonian \hat{H}_{init} , with known eigenstates that can be easily prepared on the quantum device, and a target Hamiltonian \hat{H}_{final} with unknown eigenstates.(8) A system prepared initially in an eigenstate of \hat{H}_{init} is then evolved for a total time T through the time-dependent Schrödinger equation

$$\frac{i}{T} \frac{\partial}{\partial s} |\Psi(s)\rangle = \hat{H}(s) |\Psi(s)\rangle, \quad (1)$$

where $s = t/T \in [0, 1]$ is a dimensionless path coordinate and $\hat{H}(s)$ is defined such that $\hat{H}(0) = \hat{H}_{\text{init}}$ and $\hat{H}(1) = \hat{H}_{\text{final}}$. As long as $\hat{H}(s)$ evolves sufficiently slowly along the path, and remains gapless for the eigenstate of interest, then the system will remain in an exact eigenstate for $T \rightarrow \infty$. The solution to Eq. (1) is obtained using the time-evolution operator

$$\hat{U}(s) = \mathcal{T} \left[\exp \left(\int_0^s -iT \hat{H}(s') ds' \right) \right], \quad (2)$$

where \mathcal{T} is the time-ordering operator, giving the time-evolved wavefunction $|\Psi(s)\rangle = \hat{U}(s) |\Psi(0)\rangle$. In practice, the time evolution is discretized into N steps using a first-order Trotter approximation

$$\hat{U}(s) \approx \exp \left(-i \delta s T \hat{H}(s_{N-1}) \right) \cdots \exp \left(-i \delta s T \hat{H}(s_0) \right) \quad (3)$$

where $\delta s T = \delta T$ is the time step, $\delta s = N^{-1}$, and $s_k = k/N$. The Trotter approximation becomes exact in the limit $\delta T \rightarrow 0$, while exact adiabatic evolution is achieved for $T \rightarrow \infty$. The number of steps N required to achieve satisfactory accuracy controls the quantum circuit depth and the computational cost of ASP.(8, 43, 44)

To define an adiabatic pathway that evolves a ground state into an excited state, we consider a multicomponent system where the electrons are explicitly coupled to a single two-level photon mode with frequency ω . This combined system can be described in the long-wavelength dipole limit and the length gauge using the Pauli–Fierz Hamiltonian(48)

$$\hat{H} = \hat{H}_e + \omega \hat{b}^\dagger \hat{b} - \lambda \sqrt{\frac{\omega}{2}} (\mathbf{e} \cdot \hat{\boldsymbol{\mu}}) (\hat{b}^\dagger + \hat{b}) + \frac{\lambda^2}{2} (\mathbf{e} \cdot \hat{\boldsymbol{\mu}})^2, \quad (4)$$

where the purely electronic part is defined as usual(49)

$$\hat{H}_e = V_{\text{ext}} + \sum_{pq} \hat{a}_p^\dagger \hat{a}_q h_{pq} + \frac{1}{2} \sum_{pqrs} \langle pq|rs \rangle \hat{a}_p^\dagger \hat{a}_q^\dagger \hat{a}_s \hat{a}_r. \quad (5)$$

Here, \hat{a}_p and \hat{b} are the second-quantized field operators for the electron and photon modes respectively, λ controls the electron-photon coupling strength, e is the photon polarization vector, and $\hat{\mu}$ is the electronic dipole operator. The electron-photon interaction can excite (de-excite) electrons through the dipole operator while simultaneously annihilating (creating) a photon. The last term in Eq. (4) corresponds to the dipole self-energy and is required to ensure that the Hamiltonian is bounded from below.(50) This Hamiltonian derives from the coupling of a molecule to an optical cavity, which provides a physical realization for a quantized photon field with a single mode.(50–53) In this work, the photon mode is a purely fictitious interaction used to control the adiabatic state evolution, and thus we are free to vary ω , λ , and e without physical constraints.

We describe how the electron-photon coupling can be used to adiabatically connect ground and excited states using a two-level electronic system with eigenenergies $\pm\epsilon$ and the dipole coupling $\langle \Psi_0 | e \cdot \hat{\mu} | \Psi_1 \rangle = \mu$, analogous to the Jaynes–Cummings model(54) (Fig. 1a). The diabatic basis for this system is $\{|0;0\rangle, |0;1\rangle, |1;0\rangle, |1;1\rangle\}$, where $|I;n\rangle = |I\rangle \otimes |n\rangle$ denotes the tensor product of the electronic eigenstate $|I\rangle \equiv |\Psi_I\rangle$ and a photon mode $|n\rangle$ with occupation n . The Hamiltonian in this basis is

$$\hat{H} = \begin{pmatrix} -\epsilon & 0 & 0 & \lambda\mu\sqrt{\omega/2} \\ 0 & -\epsilon + \omega & \lambda\mu\sqrt{\omega/2} & 0 \\ 0 & \lambda\mu\sqrt{\omega/2} & \epsilon & 0 \\ \lambda\mu\sqrt{\omega/2} & 0 & 0 & \epsilon + \omega \end{pmatrix}, \quad (6)$$

where the dipole self-energy $\frac{\lambda^2}{2}(e \cdot \hat{\mu})^2$ in Eq. (4) provides a uniform energy shift and can be ignored in this case. The lowest eigenstate of Eq. (6) remains almost exclusively in the diabatic state $|0;0\rangle$ for all positive ω . In contrast, in the (ω, λ) plane, the second eigenstate evolves continuously from the electronic ground state $|0;1\rangle$ for $\omega \rightarrow 0$ to the electronic excited state $|1;0\rangle$ for $\omega \gg 2\epsilon$, mirroring the annihilation of a photon during an electronic excitation (Fig. 1b). A conical intersection between the diabatic states $|0;1\rangle$ and $|1;0\rangle$ occurs at $(\omega, \lambda) = (2\epsilon, 0)$, where the electronic excitation and the photon frequency are at resonance but the coupling strength is zero. Following a suitable pathway that connects the diabatic states $|0;1\rangle$ and $|1;0\rangle$ in the (ω, λ) plane, while avoiding the conical intersection, allows the excited state to be adiabatically prepared from the ground state starting point (Fig. 1b; left).

This approach is applicable to any electronic Hamiltonian. Assuming that the ground state can be prepared on the quantum device and a suitable pathway can be defined, the first optically active excited state can be prepared without any prior knowledge of the excited-state wavefunction. Furthermore, since the fictitious photon mode is encoded as an additional qubit, post-selection on the photon qubit can be used to project the final state into the photon vacuum state, improving the fidelity of the final excited state obtained by adiabatic evolution. The definition of a suitable adiabatic pathway, and the implementation on a quantum device, are described below.

Definition of the adiabatic pathway

The adiabatic evolution $\hat{H}(s)$ for $s \in [0, 1]$ is constructed by defining parametric functions $\omega(s)$ and $\lambda(s)$. The functional forms of $\omega(s)$ and $\lambda(s)$ are constrained by the conditions $\omega(0) = 0$ and $\lambda(0) = \lambda(1) = 0$, and should be defined such that an excited state is obtained for $s = 1$. Furthermore, successful adiabatic state preparation requires that the total evolution time T satisfies the condition(8, 55)

$$T \gg \max_{K \neq J} \max_{s \in [0, 1]} \frac{|\langle \Psi_K(s) | \partial_s \hat{H}(s) | \Psi_J(s) \rangle|}{|E_K(s) - E_J(s)|^2}, \quad (7)$$

where $\{|\Psi_K(s)\rangle, E_K(s)\}$ are the instantaneous eigenpairs of $\hat{H}(s)$ and $|\Psi_J(s)\rangle$ is the eigenstate involved in the adiabatic evolution with energy $E_J(s)$. This condition derives from the probability that a non-adiabatic transition occurs and the system finishes in a different eigenstate at the end of the time evolution. The usual interpretation of this condition is that adiabatic evolution requires the target eigenstate to be non-degenerate along the full pathway, although a more precise definition is that the full fraction Eq. (7) must be near-zero everywhere.

There are three cases where $|E_K(s) - E_J(s)|$ can become small during the EXASP evolution. (i) At the avoided crossing, where the system transitions from the diabatic ground state with a photon to the excited state without a photon. In this case, the gap may be artificially widened by increasing the electron-photon coupling λ to avoid non-adiabatic transitions (Fig. 1b; right). (ii) If two eigenstate energies intersect along the pathway. From the non-crossing theorem, this can only occur if the eigenstates do not couple through $\hat{H}(s)$ due to symmetry. Since $\partial_s \hat{H}(s)$ shares the same symmetries as $\hat{H}(s)$, this implies that the numerator in Eq. (7) is zero and no non-adiabatic transition can occur between the two states. (iii) In the limit $\omega \rightarrow 0$, the initial diabatic

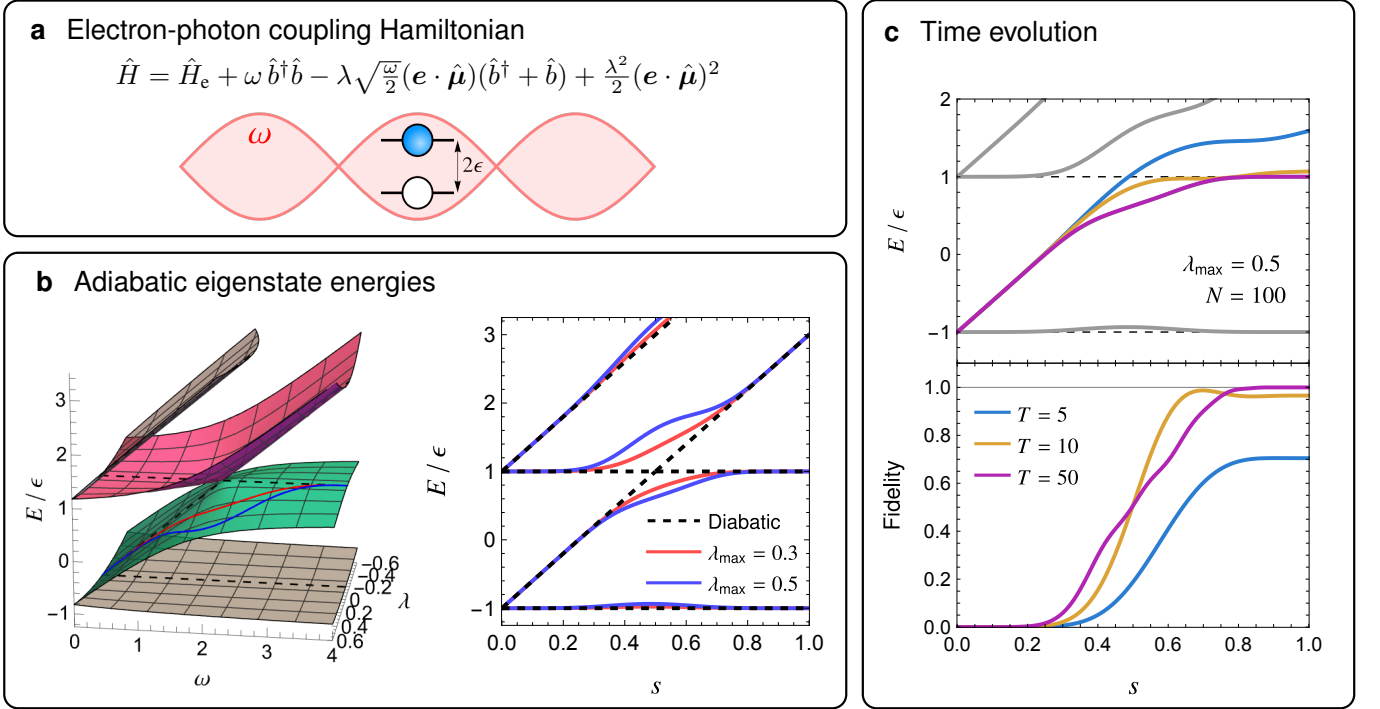


FIG. 1: Explicit electron-photon coupling enables adiabatic preparation of an excited-state wavefunction. (a) The electron-photon coupling Hamiltonian for a two-level system is analogous to the Jaynes–Cummings model. (b) The adiabatic states form a conical intersection in the (ω, λ) plane (left). Following a suitable parametrized pathway [Eq. (8)] provides a connection between the electronic ground and excited state (right), with λ_{\max} controlling the strength of the avoided crossing. (c) Adiabatic time evolution along this parametrized pathway $\hat{H}(s)$ enables the preparation of the excited-state wavefunction, with a success probability that depends on the total evolution time T .

states $|\Psi_J; 0\rangle$ and $|\Psi_J; 1\rangle$ become pairwise degenerate. If $|\Psi_0; 0\rangle$ and $|\Psi_0; 1\rangle$ are coupled through $\hat{H}(s)$, then the two states will hybridize in the $\omega \rightarrow 0$ limit to form a polaritonic state, and the excited adiabatic state preparation will become impossible. This situation occurs when the photon polarization vector transforms as the totally symmetric irreducible representation, but can be avoided using certain definitions of the path $\omega(s)$ and $\lambda(s)$, as described below.

We propose the parametrized adiabatic pathway

$$\omega(s) = \omega_{\max} s \quad \text{and} \quad \lambda(s) = \lambda_{\max} \sin^3(\pi s), \quad (8)$$

where ω_{\max} and λ_{\max} are hyperparameters and $s \in [0, 1]$. This pathway satisfies the boundary condition $\lambda(0) = \lambda(1) = 0$ and avoids forming a polaritonic state for $s \rightarrow 0$ by ensuring that the non-adiabatic coupling remains zero in this limit (Supplementary Note 1). The value of λ_{\max} can be varied to control the strength of any avoided crossings (Fig. 1b; right), while ω_{\max} must be chosen such that the avoided crossing between the ground and target excited state occurs at approximately $s = \frac{1}{2}$ (where $\lambda(s)$ is maximal). Typically this requires $\omega_{\max} \approx 2\Delta E$, where ΔE is the corresponding excitation energy that can be estimated using quantum subspace expansion or linear response theory.(30–37)

We demonstrate the full excited adiabatic state preparation for the two-level model in Eq. (4) with the electronic Hamiltonian parameters $\epsilon = 1$ and $\mu = 1$, and the path parameters $\omega_{\max} = 4$, $\lambda_{\max} = 0.5$ and $N = 100$ using a statevector simulation. Starting from the diabatic state $|0; 1\rangle$ with $E = -\epsilon$, the energy initially increases linearly as $\omega(s)$ becomes non-zero (Fig. 1c; top). Around $s = \frac{1}{2}$, there is an avoided crossing with the $|1; 0\rangle$ diabatic state and the energy plateaus at the excited-state energy $E = \epsilon$. The fidelity $|\langle 1; 0 | \Psi(s) \rangle|^2$ confirms the successful preparation of the target excited state (Fig. 1c; bottom). The accuracy of the adiabatic process improves for longer time evolution, as demonstrated by comparing the energy and fidelity for different total times $T = 5, 10$, and 50 . Since ASP is expected to be a precursor to fault-tolerant QPE, we only require a sufficiently high target fidelity, assumed to be $\sim 75\%$ in Ref. 6. The two-level system considered here demonstrates how this target fidelity for an excited state can be achieved using the EXASP procedure.

Implementation on a quantum device

To implement EXASP on real quantum hardware, we first require the initial ground state to be prepared on the quantum device. Established ground state preparation techniques can be used, such as ASP or VQE, with standard fermion-to-qubit transformations.^(56, 57) The two-level photon mode is trivially encoded using a single qubit, which is initialized in the state $|1\rangle$ to represent the ground state coupled to a photon, i.e. $|\Psi(0)\rangle = |\Psi_0\rangle \otimes |1\rangle$. A second Trotter approximation is required to implement the time-evolution steps [Eq. (3)] because $\hat{H}(s)$ generally contains non-commuting terms. This additional Trotter approximation may require a smaller time step, which we investigate in the next Section “*Optical gap for strongly-correlated Hubbard chains*”.

Once the adiabatic time evolution from $s = 0$ to 1 is complete, the quantum register is expected to be in the final state $|\Psi(1)\rangle = |\Psi_{\text{es}}\rangle \otimes |0\rangle$, where $|\Psi_{\text{es}}\rangle$ is the target electronic excited state. However, if the adiabatic evolution is not perfect, then the final state will (to a first approximation) correspond to the linear combination $|\Psi(1)\rangle \approx a |\Psi_0\rangle \otimes |1\rangle + b |\Psi_{\text{es}}\rangle \otimes |0\rangle$, where the electronic excitation has only partially occurred. The fidelity of the excited state preparation can be enhanced by using post-selection to project the final state into the photon vacuum state, with the fidelity enhancement depending on the accuracy of the adiabatic state preparation.

To investigate the performance of excited adiabatic state preparation, we consider a two-level electronic system in the non-eigenstate basis with Hamiltonian coupling g between the two basis states. The Hamiltonian and dipole operators are defined as

$$\hat{H}_e = \begin{pmatrix} -\epsilon & g \\ g & \epsilon \end{pmatrix} \quad \text{and} \quad \hat{\mu} = \begin{pmatrix} 0 & \mu \\ \mu & 0 \end{pmatrix}. \quad (9)$$

This two-level system coupled to a single two-level photon mode can be encoded using two qubits, with the Hamiltonian defined in terms of qubit Pauli operators as

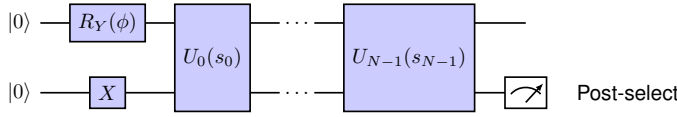
$$\hat{H}(s) = -\epsilon ZI + gXI + \frac{\omega(s)}{2}(II - IZ) - \lambda(s)\mu\sqrt{\frac{\omega(s)}{2}}XX + \frac{\lambda(s)^2\mu^2}{2}II. \quad (10)$$

The ground electronic state can be encoded using an $R_Y(\phi)$ rotation on the first qubit with $\phi = \tan^{-1}(-g/\epsilon)$, while the photon qubit is initialized in the $|1\rangle$ state (Fig. 2a). The time-evolution operator for step k is encoded with the Trotter product formula

$$\hat{U}_k(s_k) \approx e^{i\mu\lambda_k\sqrt{\frac{\omega_k}{2}}\delta T XX} e^{i\frac{\omega_k}{2}\delta T IZ} e^{-ig\delta T XI} e^{i\epsilon\delta T ZI}, \quad (11)$$

where $\omega_k = \omega(s_k)$ and $\lambda_k = \lambda(s_k)$. Constant terms in $\hat{H}(s)$ provide only a global phase-shift and can be ignored from the time evolution. The corresponding circuit implementation is shown in Fig. 2b.

a Two-level EXASP circuit



b Time evolution gate

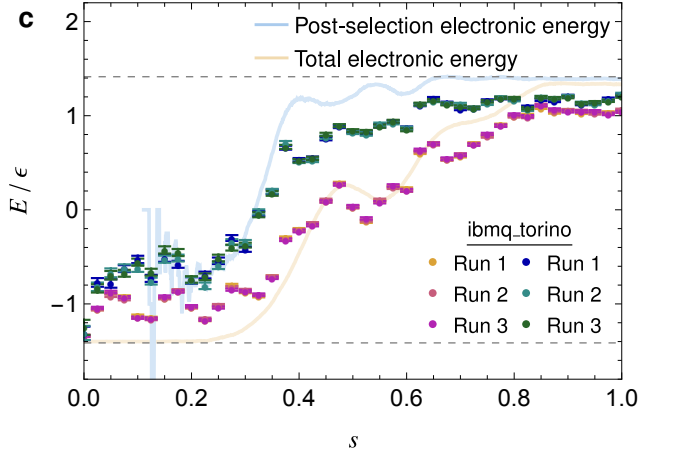
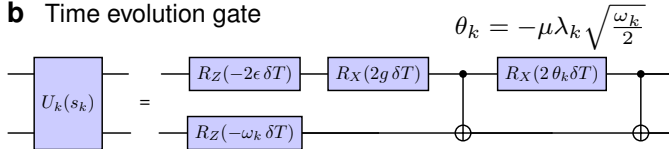


FIG. 2: Implementation of EXASP on quantum hardware for a two-level system. (a) Circuit implementation including initial ground state preparation, time-evolution gates, and post-selection for the photon vacuum state. (b) Gate decomposition of the time-evolution step for the two-level system. (c) Electronic energy expectation values for quantum hardware experiments using `ibmq_torino` with $\delta T = 0.5\epsilon^{-1}$ (points), compared to a noiseless simulation with $\delta T = 0.01\epsilon^{-1}$ (solid), showing successful adiabatic preparation of the excited state. The system parameters are $\epsilon = 1$, $g = 1$, $\mu = 1$, $T = 20$, $\omega_{\text{max}} = 5$, and $\lambda_{\text{max}} = 1$.

Simulations on near-term hardware are restricted to shallow quantum circuits, meaning that only a few adiabatic steps can be achieved. We have computed the total electronic energy (without photonic contributions) and the post-selection electronic energy along the adiabatic evolution pathway using the `ibmq_torino` quantum chip, with a total evolution time $T = 20\epsilon^{-1}$ and

$\delta T = 0.5 \epsilon^{-1}$ (Fig. 2c). These hardware results demonstrate successful adiabatic evolution from the ground state to the excited state. The time step error is evident through comparison to a noiseless simulation with $\delta T = 0.01 \epsilon^{-1}$. Initially, the post-selected electronic energy represents noise in the photon qubit state, with the electronic energy expectation value centred close to the ground-state energy. However, once the adiabatic evolution starts to evolve into the $|\Psi_{\text{es}}\rangle \otimes |0\rangle$ state, the post-selected energy converges towards the excited-state energy more rapidly than the total (unprojected) electronic energy. This faster convergence demonstrates the fidelity enhancement achieved by projecting into the zero photon state, providing a straightforward route to improve the success probability of the excited state preparation.

The non-zero time step, finite evolution time, and number of measurement shots all affect the uncertainty or accuracy of the EXASP procedure. Noisy simulations for the `ibmq_torino` quantum chip show that the measurement uncertainty in the two-level system is converged with 10^5 shots (Supplementary Figure 1). The final electronic energy estimate converges rapidly with both the total evolution time and the time step, while the photon post-selection significantly improves the accuracy for short time evolution (Fig. 3). Calculations on the `ibmq_torino` quantum chip show that current hardware noise reduces the accuracy of the final electronic energy estimate (Fig. 3). However, the adiabatic time evolution for the two-level system is simple enough that the circuit compilation reduces the excited adiabatic state preparation to only two 2-qubit gates for any T and δT (Supplementary Figure 2), meaning that the effect of noise does not grow with number of time steps in this case.

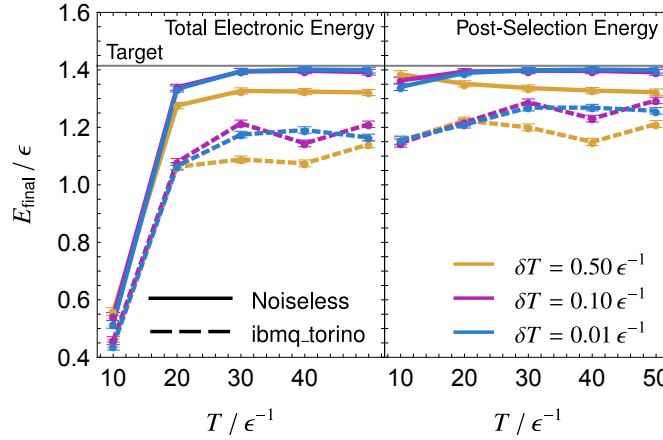


FIG. 3: **Convergence of the two-level EXASP final electronic energy with and without post-selection.** Comparison of noiseless statevector simulations with hardware calculations on the `ibmq_torino` quantum chip. Parameters used were $\epsilon = 1$, $g = 1$, $\omega_{\text{max}} = 5$, $\lambda_{\text{max}} = 1.0$, and $\mu = 1$ with 10^5 measurement shots.

Optical gap for strongly-correlated Hubbard chains

The EXASP procedure can also be applied to realistic Hamiltonians, such as the Hubbard model of strongly-correlated solid-state physics. Here, we consider a one-dimensional Hubbard chain with the electronic Hamiltonian

$$\hat{H}_e = -t \sum_{\langle p, q \rangle} (\hat{a}_{p\uparrow}^\dagger \hat{a}_{q\uparrow} + \hat{a}_{p\downarrow}^\dagger \hat{a}_{q\downarrow}) + U \sum_p \hat{n}_{p\uparrow} \hat{n}_{p\downarrow}, \quad (12)$$

where $\hat{a}_{p\sigma}^\dagger$ ($\hat{a}_{p\sigma}$) are the creation (annihilation) operators for electrons with spin σ at lattice site p , the number operators are $\hat{n}_{p\sigma} = \hat{a}_{p\sigma}^\dagger \hat{a}_{p\sigma}$, and the double sum $\sum_{\langle p, q \rangle}$ is restricted to nearest-neighbour sites (i.e., $q = p \pm 1$) with open boundary conditions. The ratio of the on-site electron repulsion U and the one-electron hopping t determines the electron correlation strength. An N -site Hubbard chain can be encoded using $2N$ qubits using the Jordan–Wigner encoding,⁽⁵⁶⁾ with an additional qubit encoding the photon state necessary for EXASP. We consider the 4- and 6-site Hubbard chains as they are sufficiently complex to explore the effects of the time step, Trotterization error, dark states, and the use of inexact starting wavefunctions on the EXASP propagation. We consider a range of correlation strengths between $U = 1t$ (weak correlation) and $U = 8t$ (strong correlation). Since these systems can be solved exactly, we always set $\omega_{\text{max}} = 2\Delta E$ using the excitation energy ΔE for the target state, and $\lambda_{\text{max}} = 1$. These parameters are found to be sufficient to give satisfactory excited state preparation.

Finding a suitable time step that is large enough to avoid long propagation times, but not so large that it introduces significant Trotterization error, is critical to adiabatic state preparation. We use the 4-site Hubbard model to investigate how the time step affects the final accuracy of the EXASP evolution. For a moderately correlated lattice ($U = 4t$) initialized with the exact ground state wavefunction, we find systematic convergence in the final state energy (including photon contributions) as the total time T increases or the time step δT decreases (Fig. 4a). The convergence with respect to T is accelerated using a smaller time step,

giving more than 96% fidelity with the target state obtained for $T = 10$ and $\delta T \leq 0.5$ when projecting onto the $|0\rangle$ photon state before measuring the energy. As expected, the accuracy of the final energy is consistently enhanced by this final state projection, with over 90% probability of successfully selecting the $|0\rangle$ photon state at $T = 10$ even though the total energy does not converge until $T \approx 20$. Therefore, post-selection on the photon vacuum state successfully accelerates the convergence of the EXASP propagation with respect to the total evolution time for realistic Hamiltonians.

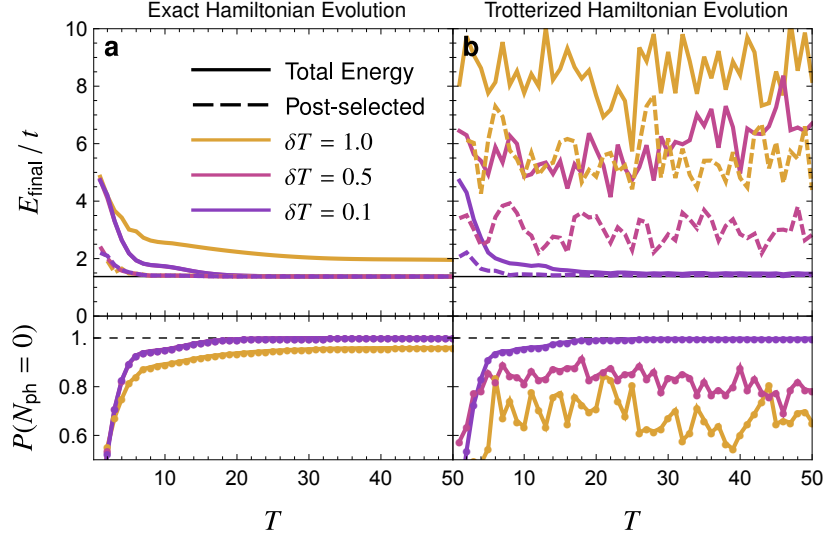


FIG. 4: **Convergence of the final energy and success probability of projecting into the $|0\rangle$ photon state for the 4-site Hubbard chain with $U = 4t$.** (a) Final energy after exact time evolution for different time steps with $U = 4t$, with and without photon state post-selection. (b) Approximating the propagation using a Trotter expansion of the time-evolution operator requires a smaller time step to obtain satisfactory convergence.

Trotterization of the time-evolution operator imposes stronger conditions on the time step to avoid excessive errors within each time-evolution step. For all the Hubbard systems considered here, $\delta T = 0.1$ is sufficiently small to allow nearly exact Trotter propagation (Fig. 4b). The observed trends for the exact Hamiltonian simulation continue to hold in this case, with convergence of the post-selected energy requiring approximately 100 applications of the time-evolution operator. In contrast, the larger time steps considered ($\delta T = 0.5$ and 1.0) lead to a final energy that does not converge in the long T limit. Notably, the time step $\delta T = 0.1$ is also sufficient to accurately propagate the 4-site Hubbard model across the entire range of correlation strengths considered (Supplementary Figure 3), as well as the larger 6-site Hubbard system (Fig. 5a). We expect that smaller time steps may be required for more complex Hamiltonians due to the presence of more non-commuting terms.

Next, we consider how the EXASP procedure changes for larger systems using the 6-site Hubbard model. As the size of the system increases, the total time required to accurately prepare an excited state also increases. For example, in the $U = 4t$ case, $T \approx 25$ is necessary for a final state fidelity greater than 96% after post-selecting the $|0\rangle$ photon state for the 6-site model, compared to $T = 10$ for 4 sites. We find that propagation for longer total time is required when the electron correlation U/t is stronger (Fig. 5a; left), and that the Trotterization error also increases with U/t (Fig. 5a; right). For example, the final state energy at $U/t = 8$ has an error of 13% that persists at large T , even after post-selection into the $|0\rangle$ photon state, suggesting that Trotterization of the time-evolution step can introduce contamination from other eigenstates that are also coupled to the $|0\rangle$ photon state.

The larger 6-site system also provides an example of how the EXASP propagation can pass over low-energy dark states to reach the first bright state, despite the presence of exact degeneracies along the adiabatic pathway. In the strongly correlated Hubbard chain, the low-lying excited states correspond to different spin arrangements where every site is singly occupied. These states have negligible dipole coupling to the antiferromagnetic ground state, meaning that they do not affect the adiabatic propagation due to the lack of nonadiabatic coupling. Instead, adiabatic state preparation with exact time propagation evolves from the ground state to the lowest-energy bright state, which includes a doubly-occupied site (Fig. 5b). Therefore, the EXASP approach naturally computes the excited-state wavefunction and energy associated with the optical gap, which is a key quantity for understanding light-matter interactions in optoelectronics and photovoltaics.

To initialize the EXASP procedure in practice, we rely on an approximate ground state prepared on the quantum device using a method such as VQE. To assess how the accuracy of this initial ground state affects the fidelity of the final excited state, we initialize the system using ground-state approximations with varying quality. We use the tiled unitary product state (tUPS) ansatz(58) for which the number of *ansatz* layers provides systematic convergence to the exact ground state. In all cases, we consider the perfect pairing tUPS (pp-tUPS) variant (see *Methods* section), which is known to converge rapidly with respect to

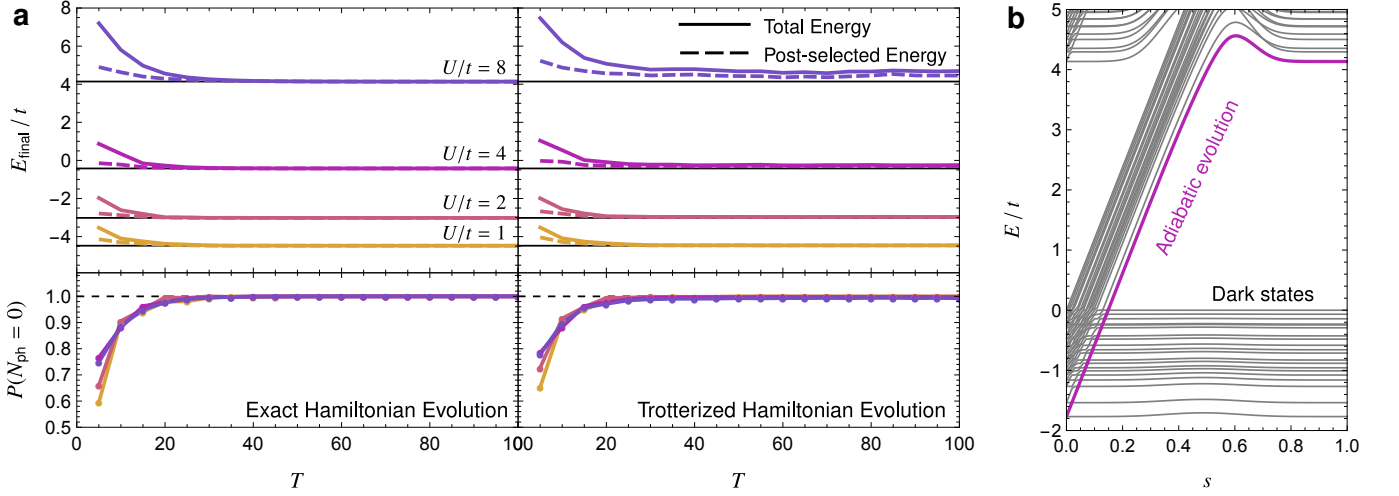


FIG. 5: **EXASP propagation for the 6-site Hubbard chain.** (a) Convergence of the final total energy and probability of measuring the $|0\rangle$ photon state at various U/t values as a function of total evolution time T with $\delta T = 0.1$. Similar convergence is obtained if the propagation is performed exactly or using a first-order Trotter expansion. (b) Adiabatic evolution along the EXASP pathway (purple) for $U/t = 8$, $T = 100$ and $\delta T = 0.1$, shown alongside the eigenvalues of the full system Hamiltonian with the dipole self-energy included (grey). EXASP leads to the first bright excited state as there is no coupling to the lower energy dark states.

the number of layers for the Hubbard model.(59) As expected, increasing the number of *ansatz* layers leads to systematically higher initial state fidelity (Supplementary Figure 4). Furthermore, for sufficiently long EXASP propagation times, the initial state fidelity error $\varepsilon_{\text{initial}} = 1 - |\langle \Psi_0 | \Psi_{\text{initial}} \rangle|^2$ is proportional to the fidelity error of the final state $\varepsilon_{\text{final}} = 1 - |\langle \Psi_J | \Psi_{\text{final}} \rangle|^2$ with the target excited state $|\Psi_J\rangle$. (Fig. 6). While the quality of a given tUPS approximation decreases as the correlation in the system increases, the relationship between the initial and final state fidelity error is independent of the correlation strength and can be fitted to a near-linear form $\varepsilon_{\text{final}} \approx 1.448\varepsilon_{\text{initial}}^{0.943}$. We note that in the long-time limit, post-selection on the photon mode has little effect on the fidelity with the target excited state, so this observed error propagation can be attributed almost exclusively to the initial state error, rather than incomplete transfer between the $|1\rangle$ and $|0\rangle$ photon states.

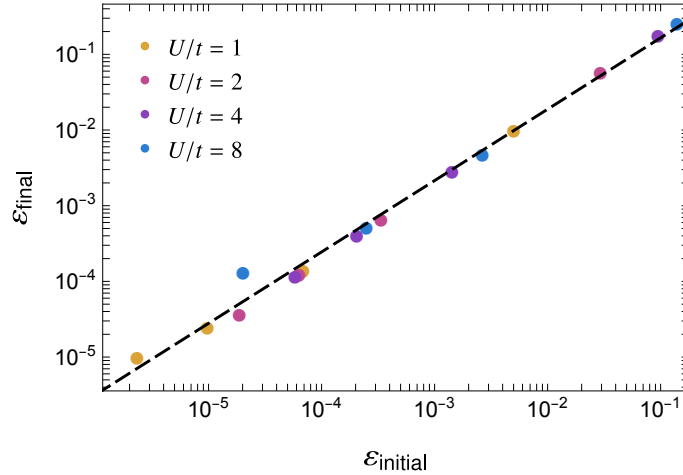


FIG. 6: **Correlation between the initial and final state fidelity error for EXASP in the 6-site Hubbard chain.** States were propagated for $T = 100$ with $\delta T = 0.1$. For each value of U/t , the different points correspond to a pp-tUPS ground state obtained with 1–4 layers, and the error decreases monotonically as the number of layers increases.

We have attempted a hardware implementation of EXASP for the two-site Hubbard model to move beyond the two-level system tested previously. This system can be mapped to three qubits if only the two-electron $m_s = 0$ subspace is considered (Supplementary Note 2). While we were able to run these calculations on the `ibmq_torino` quantum chip, the level of device noise was too high to measure any significant preparation of the excited state (Supplementary Figure 5). This result demonstrates

that current hardware is still too noisy for methods that move beyond the near-term intermediate scaling regime, such as adiabatic state preparation.

Molecular excitations using symmetry selection rules

In molecules with non-trivial point group spatial symmetry, it is often desirable to prepare excited states that transform as different irreducible representations. Targeting particular state symmetry is achieved using EXASP by changing the photon polarization vector and exploiting the dipole coupling symmetry selection rules. This approach can be illustrated for the low-lying 1^1A_1 , 1^1B_2 , and 2^1A_1 singlet states in methylene, where the molecule is oriented in the xz -plane with the principal rotation axis in the z direction. Starting the propagation in the singlet ground state, the 1^1B_2 or 2^1A_1 excited states can be systematically prepared by orienting the photon polarization vector along the y or z directions, respectively, as illustrated by the parametrized eigenstates along suitable adiabatic pathways in Fig. 7. We have numerically computed the excited-state fidelity using exact time evolution (Fig. 8), confirming that the adiabatic preparation of particular symmetry states can be achieved in practice.

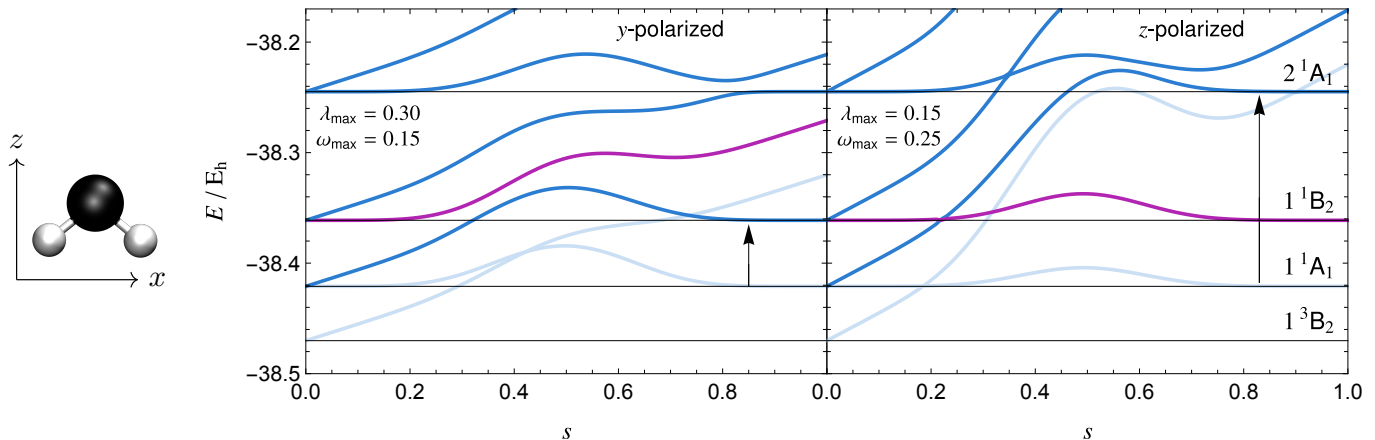


FIG. 7: **EXASP can target different excited states by varying the photon polarization vector.** Exact eigenstates of the coupled electron-photon Hamiltonian for CH_2 with a single photon mode polarized aligned along the y -direction (left) or z -direction (right). The target state (purple) evolves from the singlet ground state to the 1^1B_2 or 2^1A_1 states using the y - or z -polarization, respectively. The triplet ground state (light blue) does not couple to the singlet states and can be ignored.

Methylene also provides a molecular example to investigate how the final excited-state fidelity depends on the total time and the time step for the adiabatic evolution. The time evolution was found to be converged for a time step of $\delta T = 1.0 E_h^{-1}$. Due to the larger Hilbert space and number of Hamiltonian terms in methylene, the effect of using a Trotter approximation for each propagation step could not be feasibly tested. For the y - and z -polarized cases, total evolution times of $T = 700 E_h^{-1}$ and $T = 1300 E_h^{-1}$ are necessary to reach a target fidelity of 75 % (Fig. 8), which is considered to be sufficient to use ASP as a precursor to QPE.(6) Projection into the $|0\rangle$ photon state using post-selection significantly increases this fidelity. However, this increase in fidelity is entirely offset by the probability of measuring the $|0\rangle$ photon state, meaning that the overall probability of preparing the target excited state after QPE is the same regardless of whether photon projection is used. Nevertheless, this post-processing of the EXASP final state provides a practical route to screen for high-fidelity states. This screening allows the algorithm to fail early if post-selection fails, enhancing the success probability of a subsequent excited-state QPE calculation and minimizing the amount of wasted quantum resources. These results confirm that EXASP can be applied to selectively prepare the lowest-energy molecular excited state for different irreducible representations, which is key for applications to photochemistry.

Discussion

We have shown that excited states can be encoded on a quantum device by combining adiabatic state preparation with explicit light-matter coupling. Our EXASP algorithm prepares the lowest-energy bright state from the ground-state wavefunction by adiabatically turning on the electron-photon interaction while increasing the photon frequency. The excited-state fidelity can be further enhanced by projecting the final state into the zero-photon space using post-measurement selection on the photon qubit, providing an early failure protocol for subsequent quantum phase estimation. Furthermore, different excited states can be systematically targeted by changing the polarization direction of the photon mode. Numerical simulations demonstrate that high-fidelity excited states can be achieved for the strongly correlated Hubbard model and the methylene molecule, while experiments on current quantum hardware illustrate how the method can be implemented in practice.

EXASP offers key advantages for excited state preparation: it requires minimal information about the target excited-state wavefunction beyond an estimate of the excitation energy; it does not rely on any variational *ansatz* or modified excited-state objective function; and it avoids hybrid subspace diagonalization, which can only estimate excitation energies and would require a

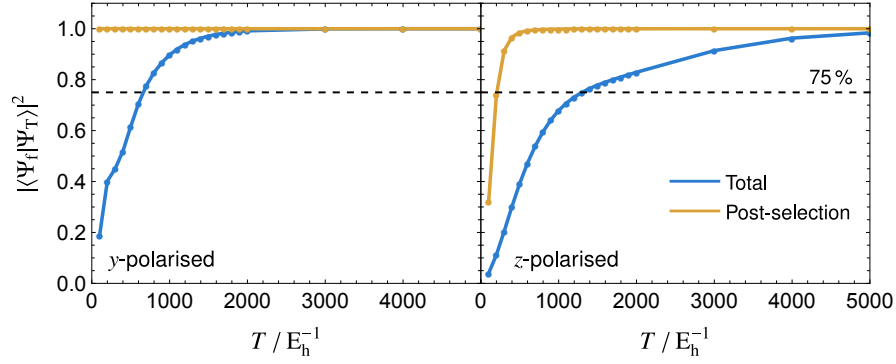


FIG. 8: **Fidelity of the excited state preparation for CH_2 systematically converges with increasing total time.** The final state fidelity is shown for $\delta T = 1.0 \text{ E}_h^{-1}$ with the photon polarization aligned along the y -direction ($\lambda_{\text{max}} = 0.30$, $\omega_{\text{max}} = 0.15$) or the z -direction ($\lambda_{\text{max}} = 0.15$, $\omega_{\text{max}} = 0.25$). Post-selection for the $|0\rangle$ photon state significantly increases the fidelity.

linear combination of unitaries to prepare an excited state on the quantum device. Furthermore, our algorithm systematically converges to the exact excited state by increasing the total time evolution and the initial state fidelity, and decreasing the time step. This systematic convergence provides a non-heuristic technique to prepare high-fidelity excited states for subsequent fault-tolerant algorithms, such as QPE or quantum dynamics. These advances lay the foundation to extend high-accuracy quantum algorithms to challenging excited states in weakly and strongly correlated electronic systems.

We have performed simulations on IBM quantum hardware to test the implementation of EXASP for model Hamiltonians. While an accurate excited-state energy can be achieved for a two-state model, the amount of hardware noise on current devices prevents any meaningful results from being obtained for more complex Hamiltonians, such as the Hubbard model. As an adiabatic evolution method, the practicality of EXASP will benefit from further advances in fault-tolerant Hamiltonian evolution and adiabatic state preparation, as well as future hardware developments. Furthermore, we have only considered the coupling of an electronic state to a single photon, which can only target the lowest-energy bright state for each optically active irreducible representation. Dark excited states with no dipole coupling to the ground state may be accessed using two or more photons, or by resetting the photon qubit to the $|1\rangle$ state at the end of the propagation and repeating the adiabatic process. We leave these extensions for future work.

The success of quantum algorithms for photophysics and photochemistry relies on the preparation of high-fidelity excited states, which is difficult to achieve with VQE or subspace expansions. Here we have shown how bright excited states can be adiabatically prepared starting from the ground state by introducing explicit light-matter coupling. The resulting EXASP methodology provides a systematically convergent approach to prepare accurate excited state wavefunctions. Our results demonstrate that adiabatic state preparation can be extended to excited electronic states, laying the foundation for future quantum algorithms to simulate light-matter interactions in molecular and materials science.

Methods

Statevector and noisy simulations

All classical simulations were performed using an in-house code implemented in python.⁽⁶⁰⁾ For the two-level model, the noiseless and noisy simulations were implemented using an interface to the QISKIT⁽⁶¹⁾ statevector simulator. Exact statevector simulations without explicit circuit sampling were performed for the 4- and 6-site Hubbard model with and without Trotterization, and for the methylene molecule. The Hamiltonian and dipole operators for the Hubbard model were defined in the site basis. For the methylene molecule, the Hamiltonian and dipole matrix elements were defined in the Hartree–Fock molecular orbital basis using the STO-3G basis set,⁽⁶²⁾ computed using the QUANTEL package.⁽⁶³⁾ Noisy simulations were performed using the AerSimulator in QISKIT with the noise model generated for the `ibmq_torino` quantum chip.

Initial ground state preparation

EXASP simulations were performed starting from the exact or an approximate ground state. The exact ground state for the two-level system was prepared using a single $R_Y(\phi)$ gate acting on the electronic qubit, with $\phi = \tan^{-1}(-g/\epsilon)$. This approach was used in both the simulated calculations and hardware implementation. For the Hubbard model and the methylene molecule, only the exact (singlet) ground state was used in statevector simulations and the circuit required to implement the ground state was ignored. The approximate ground states considered for the Hubbard model were defined using the variational perfect-paired tiled unitary product state (pp-tUPS) *ansatz*, which includes orbital optimization,⁽⁵⁸⁾ with an increasing number of layers to control

the accuracy. In this formalism, the wavefunction is defined for a reference state $|\Phi_0\rangle$ as

$$|\Psi_{\text{tUPS}}\rangle = \underbrace{\prod_{m=1}^{\lfloor N/2 \rfloor} \left(\prod_{p=1}^{\lfloor (N-1)/2 \rfloor} \hat{Q}_{2p+1,2p}^{(m)} \prod_{p=1}^{\lfloor N/2 \rfloor} \hat{Q}_{2p,2p-1}^{(m)} \right)}_{\text{orbital optimization}} \prod_{m=1}^L \left(\prod_{p=1}^{\lfloor (N-1)/2 \rfloor} \hat{U}_{2p+1,2p}^{(m)} \prod_{p=1}^{\lfloor N/2 \rfloor} \hat{U}_{2p,2p-1}^{(m)} \right) |\Phi_0\rangle, \quad (13)$$

where L is the number of layers and N is the number of spatial orbitals. The parametrized unitaries $\hat{U}_{pq}^{(m)}$ and $\hat{Q}_{pq}^{(m)}$ are given by

$$\hat{U}_{pq}^{(m)} = \exp\left(\theta_{pq,1}^{(m)} \hat{\kappa}_{pq}^{(1)}\right) \exp\left(\theta_{pq,2}^{(m)} \hat{\kappa}_{pq}^{(2)}\right) \exp\left(\theta_{pq,3}^{(m)} \hat{\kappa}_{pq}^{(1)}\right), \quad (14a)$$

$$\hat{Q}_{pq}^{(m)} = \exp\left(\theta_{pq,1}^{(m)} \hat{\kappa}_{pq}^{(1)}\right), \quad (14b)$$

where $\kappa_{pq}^{(1)} = \hat{E}_{pq} - \hat{E}_{qp}$ and $\kappa_{pq}^{(2)} = \hat{E}_{pq}^2 - \hat{E}_{qp}^2$. Here, $\hat{E}_{pq} = \hat{p}^\dagger \hat{q} + \hat{p} \hat{q}^\dagger$ is the singlet excitation operator from orbital q to p and \hat{E}_{pq}^2 is a paired double excitation from q to p . In the perfect-pairing variant of tUPS, the initial qubit register alternates between occupied and unoccupied orbitals to maximize the correlation captured by a shallow circuit, as described in Ref. 58. For our Hubbard simulations, the initial orbitals were ordered sequentially in the chain as $(\phi_1, \phi_2, \dots, \phi_N)$, where ϕ_i is the spatial orbital on site i , as this structure allows the tUPS circuit to exploit the locality of electronic interactions. The reference state $|\Phi_0\rangle$ for the pp-tUPS *ansatz* then corresponds to the Slater determinant $|\phi_1 \bar{\phi}_1 \phi_3 \bar{\phi}_3 \dots\rangle$, where the overbar denotes a low-spin orbital, although including orbital optimization reduces the dependency on the initial occupied orbitals. The optimized tUPS wavefunctions were converted to a statevector representation, which was used as the input for EXASP in place of the exact ground state.

Computation of tiled unitary product states

Following the method described in Ref. 58, the optimal parameters for the tUPS circuit were obtained through statevector simulations using global optimization with the basin hopping parallel tempering (BHPT) algorithm,(64–66) as implemented in the GMIN software.(67) This BHPT scheme used eight replica basin-hopping calculations with temperatures distributed exponentially between $0.0001 t$ and $0.01 t$, and exchange between replicas was attempted with a mean frequency of ten steps. On each basin-hopping step, the L-BFGS optimization algorithm(68–71) was performed using analytic gradients, with the convergence criteria set to a root-mean-square gradient value below $10^{-5} t$ and a maximum of 2000 iterations. A total of 250 basin hopping steps were performed for each replica and the global minimum was used to define the initial ground state.

Quantum hardware implementation

Hardware calculations for the two-level excited state preparation were performed using the `ibmq_torino` quantum chip, which is one of the IBM Quantum Heron processors. The circuit was obtained using the transpilation and optimization routines in QISKIT. Since the experiment only requires two qubits, the circuit was duplicated 50 times in parallel to maximize the use of this 133 qubit chip and maximize the number of affordable measurement shots. 200 measurement shots were performed, giving a total of 10^5 measurements using the circuit parallelization.

Data availability

The data required to reproduce figures are hosted in a publicly available repository [10.5281/zenodo.17666190]. All other data required are present in the paper or in the Supplementary Material.

Code availability

The code used to perform simulations is hosted in a public GitHub repository at <https://github.com/hgaburton/exasp.git>.

References

- [1] L. González, D. Escudero, and L. Serrano-Andrés, Progress and Challenges in the Calculation of Electronic Excited States, *Chem. Phys. Chem.* **13**, 28 (2011).
- [2] H. Lischka, D. Nachtigallová, A. J. A. Aquino, P. G. Szalay, F. Plasser, F. B. C. Machado, and M. Barbatti, Multireference Approaches for Excited States of Molecules, *Chem. Rev.* **118**, 7293 (2018).
- [3] Y. Cao, J. Romero, J. P. Olson, M. Degroote, P. D. Johnson, M. Kieferová, I. D. Kivlichan, T. Menke, B. Peropadre, N. P. D. Sawaya, S. Sim, L. Veis, and A. Aspuru-Guzik, Quantum Chemistry in the Age of Quantum Computing, *Chem. Rev.* **119**, 10856 (2019).
- [4] S. McArdle, S. Endo, A. Aspuru-Guzik, S. C. Benjamin, and X. Yuan, Quantum computational chemistry, *Reviews of Modern Physics* **92**, 15003 (2020).
- [5] M. Motta and J. E. Rice, Emerging quantum computing algorithms for quantum chemistry, *WIREs Comput. Mol. Sci.* **12**, e1580 (2022).
- [6] S. Lee, J. Lee, H. Zhai, Y. Tong, A. M. Dalzell, A. Kumar, P. Helms, J. Gray, Z.-H. Cui, W. Liu, M. Kastoryano, R. Babbush, J. Preskill, D. R. Reichman, E. T. Campbell, E. F. Valeev, L. Lin, and G. K.-L. Chan, Evaluating the evidence for exponential quantum advantage in ground-state quantum chemistry, *Nat. Comm.* **14**, 1952 (2023).

- [7] A. Aspuru-Guzik, A. D. Dutoi, P. J. Love, and M. Head-Gordon, Simulated Quantum Computation of Molecular Energies, *Science* **309**, 1704 (2005).
- [8] T. Albash and D. A. Lidar, Adiabatic quantum computation, *Rev. Mod. Phys.* **90**, 015002 (2018).
- [9] A. Peruzzo, J. McClean, P. Shadbolt, M. H. Yung, X. Q. Zhou, P. J. Love, A. Aspuru-Guzik, and J. L. O'Brien, A variational eigenvalues solver on a photonic quantum processor, *Nat. Comm.* **5**, 4213 (2014).
- [10] M. Cerezo, A. Arrasmith, R. Babbush, S. C. Benjamin, S. Endo, K. Fujii, J. R. McClean, K. Mitarai, X. Yuan, L. Cincio, and P. J. Coles, Variational quantum algorithms, *Nat. Rev. Phys.* **3**, 625 (2021).
- [11] S. Formichev, K. Hejazi, M. S. Zini, M. Kiser, J. Fraxanet, P. A. M. Casares, A. Delgado, J. Huh, A.-C. Voigt, J. E. Mueller, and J. M. Arrazola, Initial State Preparation for Quantum Chemistry on Quantum Computers, *PRX Quantum* **5**, 040339 (2024).
- [12] K. M. Nakanishi, K. Mitarai, and K. Fujii, Subspace-search variational quantum eigensolver for excited states, *Phys. Rev. Research* **1**, 033062 (2019).
- [13] R. M. Parrish, E. G. Hohenstein, P. L. McMahon, and T. J. Martínez, Quantum Computation of Electronic Transitions Using a Variational Quantum Eigensolver, *Phys. Rev. Lett.* **122**, 230401 (2019).
- [14] S. Yalouz, B. Senjean, J. Günther, F. Buda, T. E. O'Brien, and L. Visscher, A state-averaged orbital-optimized hybrid quantum–classical algorithm for a democratic description of ground and excited states, *Quantum Sci. Technol.* **6**, 024004 (2021).
- [15] H. R. Grimsley and F. A. Evangelista, Challenging excited states from adaptive quantum eigensolvers: subspace expansions vs state-averaged strategies, *Quantum Sci. Technol.* **10**, 025003 (2025).
- [16] J. R. McClean, J. Romero, R. Babbush, and A. Aspuru-Guzik, The theory of variational hybrid quantum-classical algorithms, *New J. Phys.* **18**, 023023 (2016).
- [17] R. Santagati, J. Wang, A. A. Gentile, S. Paesani, N. Wiebe, J. R. McClean, S. Morley-Short, P. J. Shadbolt, D. Bonneau, J. W. Silverstone, D. P. Tew, X. Zhou, J. L. O'Brien, and M. G. Thompson, Witnessing eigenstates for quantum simulation of Hamiltonian spectra, *Sci. Adv.* **4**, 2375 (2018).
- [18] L. Cadi Tazi and A. J. W. Thom, Folded Spectrum VQE: A Quantum Computing Method for the Calculation of Molecular Excited States, *J. Chem. Theory Comput.* **20**, 2491 (2024).
- [19] J. Lee and M. Head-Gordon, Distinguishing artificial and essential symmetry breaking in a single determinant: approach and application to the C₆₀, C₃₆, and C₂₀ fullerenes, *Phys. Chem. Chem. Phys.* **21**, 4763 (2019).
- [20] O. Higgott, D. Wang, and S. Brierley, Variational Quantum Computation of Excited States, *Quantum* **3**, 156 (2019).
- [21] H. H. S. Chan, N. Fitzpatrick, J. Segarra-Martí, M. J. Bearpark, and D. P. Tew, Molecular excited state calculations with adaptive wavefunctions on a quantum eigensolver emulation: reducing circuit depth and separating spin states, *Phys. Chem. Chem. Phys.* **23**, 26438 (2021).
- [22] Y. Ibe, Y. O. Nakagawa, N. Earnest, T. Yamamoto, K. Mitarai, Q. Gao, and T. Kobayashi, Calculating transition amplitudes by variational quantum deflation, *Phys. Rev. Research* **4**, 013173 (2022).
- [23] S. Shirai, T. Horiba, and H. Hirai, Calculation of Core-Excited and Core-Ionized States Using Variational Quantum Deflation Method and Applications to Photocatalyst Modeling, *ASC Omega* **7**, 10840 (2022).
- [24] C. Boy, M.-A. Filip, and D. J. Wales, Energy Landscapes for the Unitary Coupled Cluster Ansatz, *J. Chem. Theory Comput.* **21**, 1739 (2025).
- [25] M. Motta, W. Kirby, I. Liepuoniute, K. J. Sung, J. Cohn, A. Mezzacapo, K. Klymko, N. Nguyen, N. Yoshioka, and J. E. Rice, Subspace methods for electronic structure simulations on quantum computers, *Electron. Struc.* **6**, 013001 (2024).
- [26] N. H. Stair, R. Huang, and F. A. Evangelista, A Multireference Quantum Krylov Algorithm for Strongly Correlated Electrons, *J. Chem. Theory Comput.* **16**, 2236 (2020).
- [27] M. Motta, C. Sun, A. T. K. Tan, M. J. O'Rourke, E. Ye, A. J. Minnich, F. G. S. L. Brandão, and G. K.-L. Chan, Determining eigenstates and thermal states on a quantum computer using quantum imaginary time evolution, *Nat. Phys.* **16**, 205 (2020).
- [28] O. Oumarou, P. J. Ollitrault, C. L. Cortes, M. Scheurer, R. M. Parrish, and C. Gogolin, Molecular Properties from Quantum Krylov Subspace Diagonalization, *J. Chem. Theory Comput.* **21**, 4543 (2025).
- [29] M. G. J. ao Oliveira, Quantum block Krylov subspace projector algorithm for computing low-lying eigenenergies, *Phys. Rev. A* **112**, 052442 (2025).
- [30] J. R. McClean, M. E. Kimchi-Schwartz, J. Carter, and W. A. de Jong, Hybrid quantum-classical hierarchy for mitigation of decoherence and determination of excited states, *Phys. Rev. A* **95**, 042308 (2017).
- [31] J. I. Colless, V. V. Ramasesh, D. Dahlen, M. S. Blok, M. E. Kimchi-Schwartz, J. R. McClean, J. Carter, W. A. de Jong, and I. Siddiqi, Computation of Molecular Spectra on a Quantum Processor with an Error-Resilient Algorithm, *Phys. Rev. X* **8**, 011021 (2018).
- [32] P. J. Ollitrault, A. Kandala, C.-F. Chen, P. K. Barkoutsos, A. Mezzacapo, M. Pistoia, S. Sheldon, S. Woerner, J. M. Gambetta, and I. Tavernelli, Quantum equation of motion for computing molecular excitation energies on a noisy quantum processor, *Phys. Rev. Research* **2**, 043140 (2020).
- [33] M. Urbanek, D. Camps, R. V. Beeumen, and W. A. de Jong, Chemistry on Quantum Computers with Virtual Quantum Subspace Expansion, *J. Chem. Theory Comput.* **16**, 5425 (2020).
- [34] A. Asthana, A. Kumar, V. Abraham, H. Grimsley, Y. Zhang, L. Cincio, S. Tretiak, P. A. Dub, S. E. Economou, E. Barnes, and N. J. Mayhall, Quantum self-consistent equation-of-motion method for computing molecular excitation energies, ionization potentials, and electron affinities on a quantum computer, *Chem. Sci.* **14**, 2405 (2023).
- [35] P. W. K. Jensen, E. R. Kjellgren, P. Reinholdt, K. M. Ziems, S. Coriani, J. Kongsted, and S. P. A. Sauer, Quantum Equation of Motion with Orbital Optimization for Computing Molecular Properties in Near-Term Quantum Computing, *JCTC* **20**, 3613 (2014).
- [36] P. Reinholdt, E. R. Kjellgren, J. H. Fuglsbjerg, K. M. Ziems, S. Coriani, S. P. A. Sauer, and J. Kongsted, Subspace Methods for the Simulation of Molecular Response Properties on a Quantum Computer, *J. Chem. Theory Comput.* **20**, 3729 (2024).
- [37] A. Gandon, A. Baiardi, P. Ollitrault, and I. Tavernelli, Nonadiabatic Molecular Dynamics with Fermionic Subspace-Expansion Algorithms on Quantum Computers, *J. Chem. Theory Comput.* **20**, 5951 (2024).

- [38] K. Kanno, M. Kohda, R. Imai, S. Koh, K. Mitarai, W. Mizukami, and Y. O. Nakagawa, Quantum-selected configuration interaction: classical diagonalization of hamiltonians in subspaces selected by quantum computers (2023), [arXiv:2302.11320v1](#).
- [39] P. Reinholdt, K. M. Ziemis, E. R. Kjellgren, S. Coriani, S. P. A. Sauer, and J. Kongsted, Critical Limitations in Quantum-Selected Configuration Interaction, **2025** **21**, 6811 (2025).
- [40] M. Mikkelsen and Y. O. Nakagawa, Quantum-selected configuration interaction with time-evolved state, **Phys. Rev. Research** **7**, 043043 (2025).
- [41] J. Robledo-Moreno, M. Motta, H. Haas, A. Javadi-Abhari, P. Jurcevic, W. Kirby, S. Martiel, K. Sharma, S. Sharma, T. Shirakawa, I. Sitdikov, R.-Y. Sun, K. J. Sung, M. Takita, M. C. Tran, S. Yunoki, and A. Mezzacapo, Chemistry beyond the scale of exact diagonalization on a quantum-centric supercomputer, **Sci. Adv.** **11**, eadu9991 (2025).
- [42] S. Barison, J. R. Moreno, and M. Motta, Quantum-centric computation of molecular excited states with extended sample-based quantum diagonalization, **Quantum Sci. Technol.** **10**, 025034 (2025).
- [43] L. Veis and J. Pittner, Adiabatic state preparation study of methylene, **J. Chem. Phys.** **140**, 214111 (2014).
- [44] V. Kremenetski, C. Mejuto-Zaera, S. J. Cotton, and N. M. Tubman, Simulation of adiabatic quantum computing for molecular ground states, **J. Chem. Phys.** **155**, 234106 (2021).
- [45] E. Granet, K. Ghanem, and H. Dreyer, Practicality of a quantum adiabatic algorithm for chemistry applications, **Phys. Rev. A** **111**, 022428 (2025).
- [46] D. Marti-Dafcik, H. G. A. Burton, and D. P. Tew, Spin coupling is all you need: Encoding strong electron correlation in molecules on quantum computers, **Phys. Rev. Research** **7**, 013191 (2025).
- [47] M. Born and V. Fock, Beweis des Adiabatsatzes, **Z. Phys.** **51**, 165 (1928).
- [48] H. Spohn, *Dynamics of Charged Particles and their Radiation Field* (Cambridge University Press, Cambridge, 2004).
- [49] T. Helgaker, P. Jørgensen, and J. Olsen, *Molecular Electronic-Structure Theory* (John Wiley & Sons, 2000).
- [50] V. Rokaj, D. M. Welakuh, M. Ruggenthaler, and A. Rubio, Light-matter interaction in the long-wavelength limit: no ground-state without dipole self-energy, **J. Phys. B: At. Mol. Phys.** **51**, 034005 (2018).
- [51] U. Mordovina, C. Bungey, H. Appel, P. J. Knowles, A. Rubio, and F. R. Manby, Polaritonic coupled-cluster theory, **Phys. Rev. Research** **2**, 023262 (2020).
- [52] T. S. Haugland, E. Ronca, E. F. Kjønsstad, A. Rubio, and H. Koch, Coupled Cluster Theory for Molecular Polaritons: Changing Ground and Excited States, **Phys. Rev. X** **10**, 041043 (2020).
- [53] M. Ruggenthaler, D. Sidler, and A. Rubio, Understanding Polaritonic Chemistry from Ab Initio Quantum Electrodynamics, **Chem. Rev.** **123**, 11191 (2023).
- [54] E. T. Jaynes and F. W. Cummings, Comparison of quantum and semiclassical radiation theories with application to the beam maser, **Proc. IEEE** **51**, 89 (1963).
- [55] M. H. S. Amin, Consistency of the Adiabatic Theorem, **Phys. Rev. Lett.** **102**, 220401 (2009).
- [56] P. Jordan and E. Wigner, Über das Paulische Äquivalenzverbot, **Z. Phys.** **47**, 631 (1928).
- [57] S. B. Bravyi and A. Y. Kitaev, Fermionic Quantum Computation, **Ann. Phys.** **298**, 210 (2002).
- [58] H. G. A. Burton, Accurate and gate-efficient quantum ansätze for electronic states without adaptive optimization, **Phys. Rev. Research** **6**, 023300 (2024).
- [59] H. G. A. Burton, Tiled unitary product states for strongly correlated Hamiltonians, **Faraday Discuss.** **254**, 157 (2024).
- [60] H. G. A. Burton, EXASP, <https://github.com/hgaburton/exasp> ().
- [61] A. Javadi-Abhari, M. Treinish, K. Krsulich, C. J. Wood, J. Lishman, J. Gacon, S. Martiel, P. D. Nation, L. S. Bishop, A. W. Cross, B. R. Johnson, and J. M. Gambetta, **Quantum computing with qiskit** (2024), [arXiv:2405.08810 \[quant-ph\]](#).
- [62] W. J. Hehre, R. F. Stewart, and J. A. Pople, Self-Consistent Molecular-Orbital Methods. I. Use of Gaussian Expansions of Slater-Type Atomic Orbitals, **J. Chem. Phys.** **51**, 2657 (1969).
- [63] H. G. A. Burton, QUANTEL, <https://github.com/hgaburton/quantel> ().
- [64] B. Strodel, J. W. L. Lee, C. S. Whittleston, and D. J. Wales, Transmembrane structures for alzheimer's α 1-42 oligomers, **J. Am. Chem. Soc.** **132**, 13300 (2010).
- [65] Z. Li and H. A. Scheraga, Monte carlo-minimization approach to the multiple-minima problem in protein folding, **PNAS** **84**, 6611 (1987).
- [66] D. J. Wales and J. P. K. Doye, Global Optimization by Basin-Hopping and the Lowest Energy Structures of Lennard-Jones Clusters Containing up to 110 Atoms, **J. Phys. Chem. A** **101**, 5111 (1997).
- [67] GMIN: A program for finding global minima and calculating thermodynamic properties, <http://www-wales.ch.cam.ac.uk/software.html>.
- [68] C. G. Broyden, The Convergence of a Class of Double-rank Minimization Algorithms 1. General Considerations, **IMA J. Appl. Math.** **6**, 76 (1970).
- [69] R. Fletcher, A new approach to variable metric algorithms, **Comput. J.** **13**, 317 (1970).
- [70] D. Goldfarb, A family of variable-metric methods derived by variational means, **Math. Comp.** **24**, 23 (1970).
- [71] D. F. Shanno, Conditioning of quasi-Newton methods for function minimization, **Math. Comp.** **24**, 647 (1970).

Acknowledgements

H.G.A.B. was supported by Downing College, Cambridge through the Kim and Julianna Silverman Research Fellowship and is a Royal Society University Research Fellow (URFAR0\241299) at University College London. M.A.F. acknowledges financial support from Peterhouse College, Cambridge through a Research Fellowship. We acknowledge the use of IBM Quantum services for this work. The views expressed are those of the authors, and do not reflect the official policy or position of IBM or the IBM Quantum team.

Author contributions

H.G.A.B. conceived the project and managed the collaboration. H.G.A.B. and M.A.F. jointly designed and implemented the code, carried out numerical simulations, performed the data analysis, and contributed to preparing and reviewing the manuscript.

Competing interests

The authors declare no competing interests.